A HYBRID 3D MICRO-NANOPRINTING APPROACH FOR BIOMEDICAL MICROINJECTION NEEDLE ARRAYS

Sunandita Sarker[1,], Adira Colton[1], Ziteng Wen[1], Xin Xu[1], Piotr Walczak[2], Miroslaw Janowski[2], Yajie Liang[2] and Ryan D. Sochol[1]*
[1]University of Maryland, College Park, MD, USA
[2]University of Maryland School of Medicine, Baltimore, MD, USA

ABSTRACT

Microinjection protocols are critical to biomedical research and clinical applications, including for the delivery of emerging stem cell therapies that hold distinctive promise for treating neurodegenerative diseases. One pervasive challenge inherent to using traditional microneedles for such stem cell therapies, however, is that, because there is typically only a single opening at the tip, either: (*i*) too many cells are injected as a spheroid, which limits nutrients from reaching the interior stem cells, leading to undesired cell death; or (*ii*) not enough cells are injected to educe a therapeutic response. To provide a pathway that could ultimately bridge this gap, here we investigate a hybrid additive manufacturing (or "three-dimensional (3D) printing") approach to realize microneedle arrays at scales that are relevant and advantageous for microinjection into the brain. Specifically, we leverage "*ex situ* Direct Laser Writing (*es*DLW)" to 3D nanoprint arrays of 50 μm-in-diameter microneedles directly onto Digital Light Processing (DLP) 3D-microprinted capillaries. Microfluidic cyclic burst-pressure testing for input pressures up to 275 kPa (n = 100) revealed uncompromised fluidic integrity at the array-capillary interface. *Ex vivo* experiments performed on an excised mouse brain revealed that the microneedle arrays could not only withstand penetration into the tissue, but also yield effective microinjection of a surrogate fluid into the brain. In combination, these results suggest that the presented microneedle array strategy offers unique potential for biomedical microinjection applications.

KEYWORDS

Additive Manufacturing, 3D Printing, Direct Laser Writing, Two-Photon Polymerization, Digital Light Processing

INTRODUCTION

Microinjection technologies are widely employed in both research settings (*e.g.*, for developmental biology and transgenics) and clinical applications ranging from *in vitro* fertilization to intraocular injection [1–3]. For example, researchers have found that targeted microinjection of therapeutic drugs can improve the efficacy of treatments for cancer as well as for autoimmune and infectious diseases [4–5]. Among emerging medical treatments, one particular microinjection application that has garnered increasing attention is stem cell-based therapy—a class of medical procedures that involve the targeted microinjection of stem cells to repair damaged tissue (*e.g.*, in the spinal cord, brain, and joints) or improve a weakened immune system [6, 7]. Previously, we demonstrated the potential of stem cell therapies for treating neurological disorders [8, 9]. Yet, the efficacy of such treatments remains highly dependent on the underlying microinjection process, which significantly affects the survival of transplanted cells as well as the overall therapeutic efficacy [10, 11]. For example, if the number of stem cells injected is too large, then nutrient transport to cells located in interior regions can be obstructed, resulting in cell death [12, 13]. Conversely, if too few cells are injected, then—despite the likelihood of cell survival—the therapeutic effect will be limited [14]. Thus, new microinjection strategies are in critical demand.

CONCEPT

A shift from traditional microinjection needles that comprise a singular output port to microneedle arrays (with many output ports) offers a promising means to overcome the aforementioned microinjection-associated deficits for stem cell-based therapies. Although researchers have demonstrated the utility of mesoscale needle arrays for distributing drugs or target cells uniformly to a large area with minimal tissue damage [15,16], neurological stem cell therapies necessitate markedly higher injection densities (*e.g.*, 100–200 μm center-to-center needle spacing) and high-aspect-ratio needle tips (*e.g.*, >600 μm heights, 50 μm diameters). In addition, such arrays must be fabricated at the end of fluidic capillaries, which presents a considerable challenge for conventional microfabrication methods. Recently, we reported an "*ex situ* Direct Laser Writing (*es*DLW)" strategy for printing 3D microfluidic structures directly onto—and notably, fully sealed to—fluidic tubing that can be manipulated by hand [17], and then demonstrated this approach for microinjection needles with a singular tip [18]. In this work, we advance this *es*DLW concept, while remediating its alignment-associated drawbacks, to introduce a novel hybrid additive manufacturing strategy

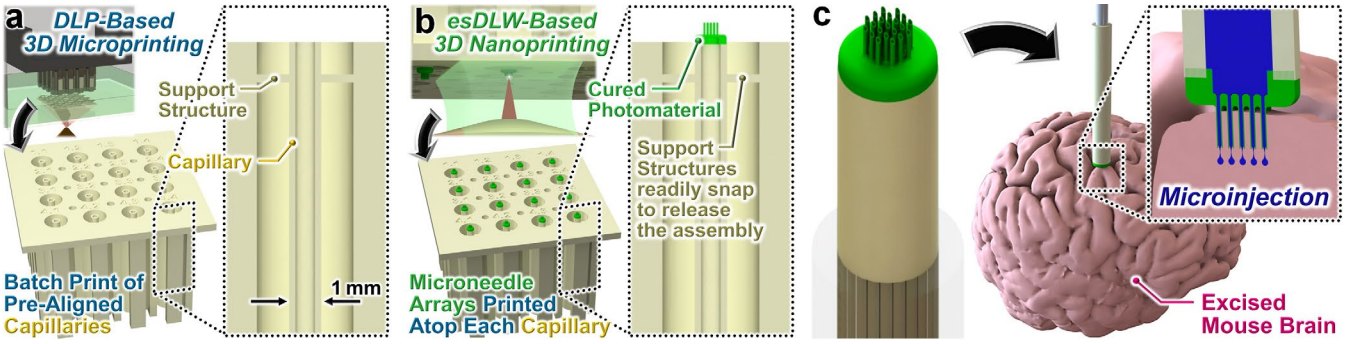

Figure 1: *Conceptual overview of the hybrid 3D micro-nanoprinting strategy for additively manufacturing microinjection needle arrays.* ***(a)*** *Digital Light Processing (DLP)-based 3D microprinting of 16 pre-aligned capillaries.* ***(b)*** *"Ex situ Direct Laser Writing (esDLW)"-based 3D nanoprinting of microneedle arrays directly atop—and fluidically sealed to—each capillary.* ***(c)*** *Individual microneedle array (after selective release by manually pushing the opposing side of a target capillary to break the thin supporting structures) integrated with an injector system to support the delivery of biomedical payloads (e.g., therapeutic drugs and/or stem cell suspensions) into the brain.*

978-1-940470-04-7/HH2022/$25©2022TRF
DOI 10.31438/trf.hh2022.6

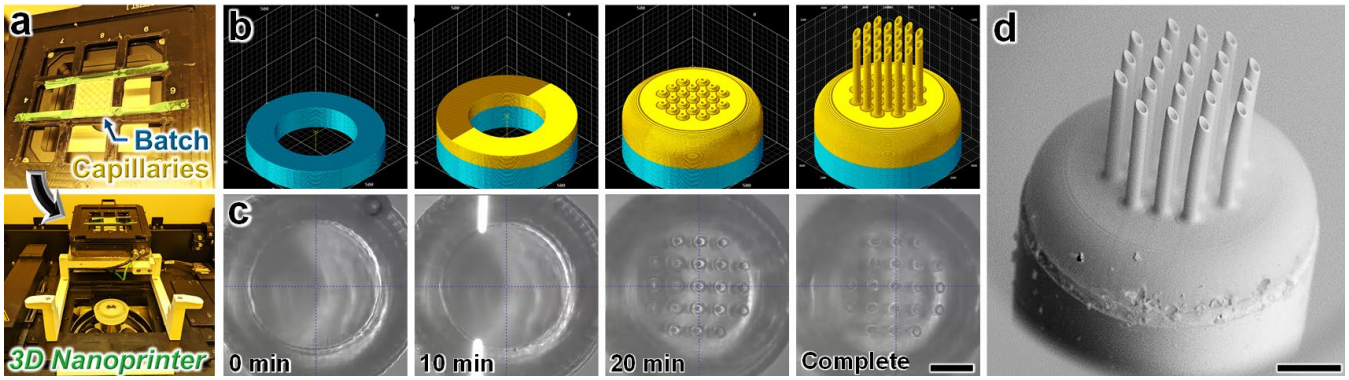

Figure 2: *Fabrication results.* ***(a)*** *DLP-printed batch capillaries loaded into the DLW 3D nanoprinter.* ***(b, c)*** *Computer-aided manufacturing (CAM) simulations* ***(b)*** *and corresponding micrographs* ***(c)*** *of the esDLW process for 3D nanoprinting a complete microneedle array directly onto a capillary in a single print run.* ***(d)*** *SEM micrograph of a fabricated microneedle array-capillary assembly. Scale bars = 200 μm*

for 3D nanoprinting microinjection needle arrays atop 3D-micro-printed capillaries to ultimately support stem cell therapies (**Fig. 1**).

The hybrid 3D micro-nanoprinting strategy consists of three fundamental steps. First, DLP-based 3D microprinting—a vat photopolymerization approach in which a photocurable material is selectively crosslinked layer by layer to produce 3D objects—is used to fabricate a batch of capillaries in designated array positions (**Fig. 1a**). In contrast to our prior works that required custom-built capillary holders that relied on undesired manual (*i.e.*, by hand/eye) alignment protocols [17, 18], batch printing of the capillaries allows for facile loading into the 3D nanoprinter with all capillaries in pre-defined positions and orientations. The second step entails *es*DLW printing of the microneedle arrays directly onto the tops of the DLP-printed capillaries. To do so, photomaterial is dispensed atop a capillary, and then a femtosecond pulsed IR laser is scanned in a point-by-point, layer-by-layer manner to selectively crosslink the photomaterial in target locations *via* two-photon (or multi-photon) polymerization phenomena (**Fig. 1b**). In the final step, individual microneedle array-capillary assemblies can be selectively released from the batch—*i.e.*, by manually pushing the opposing side of the capillary to break the thin support structures (**Fig. 1b – *inset***). Thereafter, the opposing end of the capillary can be interfaced with fluidic tubing or injector systems to facilitate the delivery of biomedical fluidic payloads (*e.g.*, therapeutic drugs and/or stem cell suspensions) into target sites, such as the brain (**Fig. 1c**).

MATERIALS AND METHODS

Digital Light Processing (DLP)-Based 3D Microprinting of the Pre-Aligned Capillaries in Batch

The computer-aided design (CAD) software, SolidWorks (Dassault Systèmes, France), was used to generate models of batch arrays of 16 capillaries. Each capillary was designed with an inner diameter (ID) of 500 μm and an outer diameter (OD) of 1 mm. Models were exported as STL files and imported into the slicer tool for the Miicraft M50 DLP 3D printer (CADworks3D, Canada). Capillary batches were printed using Clear Microfluidic Resin v7.0a (CADworks) with the layer height set to 50 μm. Following the DLP process, the prints were developed in methanol for approximately 10 s, and then methanol was perfused through each capillary to eliminate any residual resin from the interiors. Lastly, the prints were dried with pressurized air and cured under UV light for 10 s.

Ex Situ Direct Laser Writing (*es*DLW)-Based 3D Nanoprinting of Microneedle Arrays onto the Capillaries

The microneedle arrays—modeled with SolidWorks (Dassault Systèmes)—each comprised 21 identical needle tips (ID = 30 μm; OD = 50 μm; height = 700 μm). The models were exported as STL files and imported into the computer-aided manufacturing (CAM) software, DeScribe (Nanoscribe GmbH, Karlsruhe, Germany). The print settings included a hatching distance of 700 nm and a layer height of 2.5 μm. Initially, IP-Q photoresist (Nanoscribe) was dispensed atop the capillaries, and the batch assembly was loaded into the Nanoscribe Photonic Professional GT2 3D printer (**Fig. 2a**). For *es*DLW printing, the Dip-in Laser Lithography (DiLL) mode was used with a 10× objective lens, a laser power of 27.5 mW, and a laser scanning speed of 120,000 μm/s. The printing process was initiated with 50 μm of overlap with the top capillary surfaces. Following the *es*DLW process, the batch assembly was removed from the printer and developed using propylene glycol methyl ether acetate (PGMEA) for 60 min and isopropyl alcohol (IPA) for 5 min, and then allowed to dry under ambient conditions. Lastly, target microneedle array-capillary assemblies were manually released from the batch by pushing the opposing end of the capillary to yield complete detachment from the support structure connections.

Optical Characterization

All scanning electron microscope (SEM) images were captured using a TM4000 Tabletop SEM (Hitachi, Tokyo, Japan). Brightfield microscopy during microfluidic testing was performed using an inverted microscope (Motic AE31, Motic, Canada) connected to a charge-coupled device (CCD) camera (Moticam Pro 285B, Motic). For *ex vivo* microinjection experiments, optical characterizations were performed using the Monocular Max 300x microscope objective and a 41MP USB C-Mount Industry Microscope Camera Set (Hayear Electronics Co. Ltd., Shenzhen, China).

Microfluidic Experimentation

Fluidic testing was performed using the Fluigent Microfluidic Control System MFCS and OxyGEN software (Fluigent, France). DI water was inputted *via* fluidic tubing connected to the opposing end of the capillaries. Three separate sets of cyclic burst-pressure experiments were performed corresponding to applied pressures of approximately 75 kPa, 175 kPa, and 275 kPa for 5 s, but then set to 0 kPa for 5 s after each pressure increase for all cases. Each set of experiments were performed for n = 100 cycles while the microneedle array-capillary interface was monitored for potential signs of undesired leakage phenomena (*e.g.*, fluid exiting at points along the interface rather than out the tops of the microneedle tips).

Ex Vivo Mouse Brain Microinjection Experimentation

Brain tissue excised from a six-month-old male mouse (Wild-type C57BL/6 J, Jackson Laboratory) was used for *ex vivo* microinjection experiments. The brain with an intact dura mater was excised within 10 min of euthanasia and stored in phosphate-

buffered saline (PBS) (Sigma-Aldrich, Saint Louis, MO) on ice prior to testing. The tissue sample was handled gently before and during the experiment to maintain tissue integrity. The microneedle array-capillary assembly was interfaced with a custom-built nanoinjector (Narashige, MO10) to control the displacement and to perform microinjections with a surrogate fluid (blue-dyed DI water).

RESULTS AND DISCUSSION

Hybrid 3D Micro-Nanoprinting-Based Fabrication

The total DLP printing process was completed in 45 minutes, with the resulting batch capillaries resolved with overall dimensions that allowed for facile loading into the DLW 3D printer (**Fig. 2a**). CAM simulations and corresponding micrographs of the *es*DLW process for 3D printing a microneedle array directly onto a DLP-printed capillary are presented in **Figure 2b** and **2c**, respectively. The total *es*DLW printing process was completed within 25 minutes. SEM micrographs of fabrication results revealed effective alignment and integration of the microneedle arrays with the capillaries, without any signs of defects along the interface (*e.g.*, **Fig. 2d**).

Microfluidic Burst-Pressure Characterization

To investigate the mechanofluidic integrity of the microneedle array-capillary interface, we connected the opposing end of the capillaries to fluidic adapters (**Fig. 3a**) and performed cyclic burst-pressure tests while optically monitoring the microneedle array. Experimental results did not reveal any signs of undesired leakage phenomena (*e.g.*, fluid exiting *via* the interface rather than out of the needle tips) (**Fig. 3b**). In addition, quantified results for cyclic burst-pressure testing up to 275 kPa—notably higher that prior targets of 70 kPa [16]—similarly revealed uncompromised fluidic integrity, as evidenced by the flow rate returning to a consistent magnitude after each ramp up in applied pressure for all cases (*e.g.*, **Fig. 3c–e**).

Ex Vivo Mouse Brain Microinjection

Two sets of *ex vivo* experiments were performed with a brain excised from a euthanized mouse (**Fig. 4a**). As a fundamental measure of microneedle array efficacy, we initially investigated the ability to successfully penetrate the brain tissue without mechanical failure (*e.g.*, needle tip fracture). The microneedle array-capillary assembly was interfaced with a nanoinjector to facilitate controlled insertion while monitoring the displacement (*e.g.*, **Fig. 4b**). After a total displacement of 1 mm, the microneedle array was retracted, and the process was repeated twice more. SEM micrographs of the microneedle arrays following these repeated tissue puncture experiments did not reveal any signs of mechanical failure (*e.g.*, **Fig. 4c**).

To investigate the biomedical microinjection capability of the printed microneedle array, we loaded the microneedle array-capillary assembly with a surrogate fluid and then interfaced the assembly with the nanoinjector (**Fig. 4a**). Akin to the tissue penetration experiments, we used the nanoinjector to insert the microneedle array into the brain tissue, but in this case, we then used the pneumatically controlled nanoinjector to deliver the surrogate fluid into the tissue (**Fig. 4d**). After retracting the microneedle array, we washed the surface of the injection site with PBS to eliminate any residual fluid from the surface. Subsequent optical characterizations revealed successful penetration and microinjection of the surrogate fluid into the brain tissue (*e.g.*, **Fig. 4e**).

CONCLUSION

Microinjection protocols underlie a diversity of applications in biomedical fields, yet traditional microneedle architectures with singular tips suffer from limited utility, such as for stem cell therapy. In this work, we presented a novel hybrid additive manufacturing strategy for printing microinjection needle arrays at scales that are

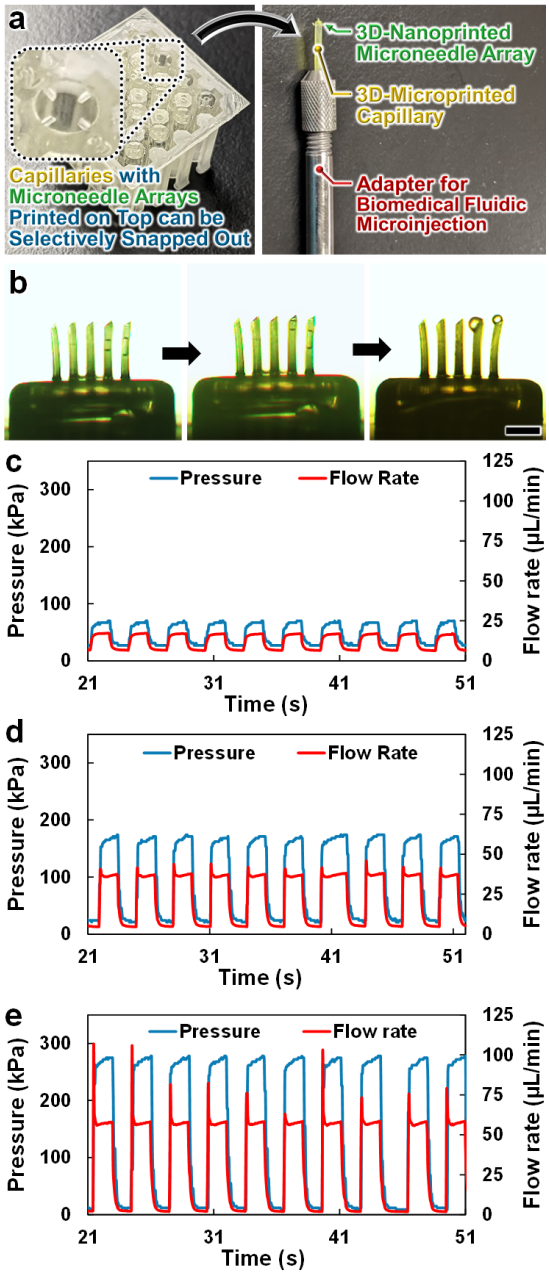

Figure 3: *Experimental results for microfluidic characterizations.* ***(a)*** *Example of a microneedle array-capillary assembly individually released from the batch and then interfaced with an adapter for fluidic loading.* ***(b)*** *Sequential micrographs during fluidic infusion. Scale bar = 200 µm.* ***(c–e)*** *Results for cyclic burst-pressure testing with DI water during representative intervals for input pressure cycles targeting:* ***(c)*** *75 kPa;* ***(d)*** *175 kPa; and* ***(e)*** *275 kPa.*

relevant and beneficial for emerging stem cell therapies for treating neurological disorders. Specifically, we combined DLP-based 3D printing with our *es*DLW approach to print microneedle arrays capable of withstanding 275 kPa pressure cycling and repeated insertion into an excised mouse brain. Notably, the demonstrated *ex vivo* microinjection of a surrogate fluid into a mouse brain represents a critical proof of principle for the presented strategy to offer utility for stem cell therapy. While future efforts should focus on interrogating the efficacy of the microneedle arrays for the delivery of stem cell suspensions, the current results for the presented

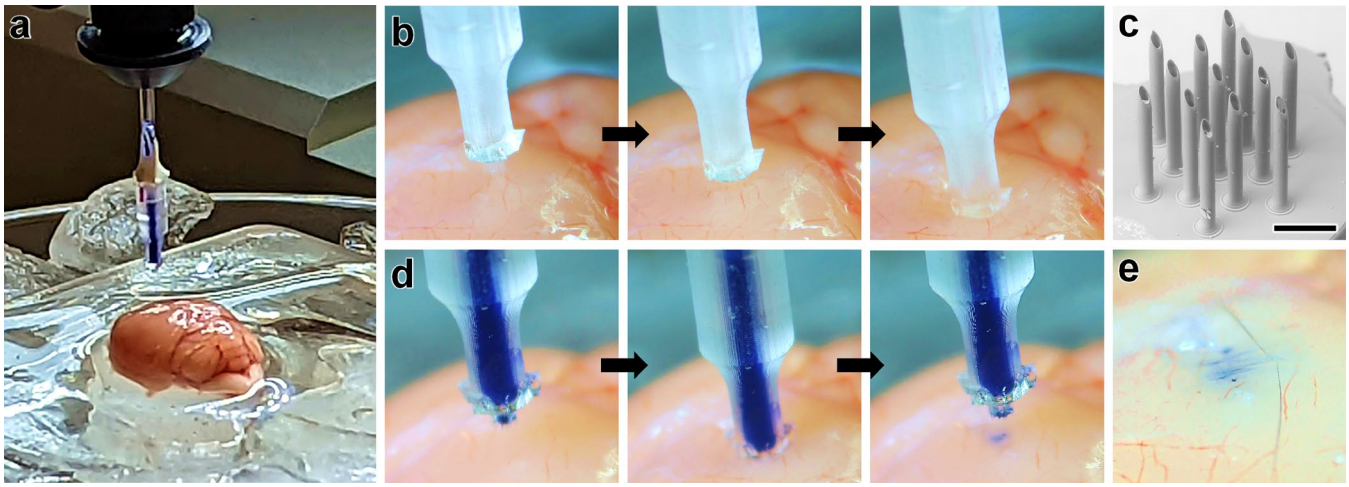

Figure 4: *Experimental results for ex vivo microinjection into an excised mouse brain.* ***(a)*** *Experimental setup for microneedle array-capillary assembly interfaced with a custom-built nanoinjector.* ***(b,c)*** *Tissue puncture results.* ***(b)*** *Sequential images during microneedle array insertion into brain tissue.* ***(c)*** *SEM micrograph of microneedle array after retraction from the brain tissue. Scale bar = 200 µm.* ***(d,e)*** *Microneedle array-based microinjection results for a surrogate fluid (blue-dyed DI water).* ***(d)*** *Sequential images before (left), during (middle), and after (right) microinjection into brain tissue.* ***(e)*** *Expanded view of the post-injection site.*

strategy serve as a critical foundation as an enabling technology for new microinjection applications that promote human health.

ACKNOWLEDGEMENTS

We greatly appreciate the contributions of members of the Bioinspired Advanced Manufacturing (BAM) Laboratory and the technical staff of Terrapin Works as well as the Robert E. Fischell Institute for Biomedical Devices at the University of Maryland, College Park.

REFERENCES

[1] J. Puschhof, *et al.*, "Intestinal organoid cocultures with microbes", *Nature Protocol,* 16, (2021).

[2] S. Rafiq, C.S. Hackett, R.J. Brentjens, "Engineering strategies to overcome the current roadblocks in CAR T cell therapy", *Nature Reviews Clinical Oncology,* 17 (2020).

[3] C. Askew et al., "Tmc gene therapy restores auditory function in deaf mice", *Science Translational Medicine,* 7 (2015).

[4] M. Halasz, *et al.*, "Integrating network reconstruction with mechanistic modeling to predict cancer therapies", *Science Signaling,* 9 (2016).

[5] Y. Oda *et al.*, "Discovery of anti-inflammatory physiological peptides that promote tissue repair by reinforcing epithelial barrier formation", *Science Advances,* 7 (2021).

[6] F.K. Wong, *et al.*, "Microinjection of membrane-impermeable molecules into single neural stem cells in brain tissue", *Nature Protocol*, 9 (2014).

[7] M.H. Amer *et al.*, "Translational considerations in injectable cell-based therapeutics for neurological applications: concepts, progress and challenges, *NPJ Regenerative Medicine,* 2 (2017).

[8] Y. Liang, L. Ågren, A. Lyczek, P. Walczak, J.W.M. Bulte, "Neural progenitor cell survival in mouse brain can be improved by co-transplantation of helper cells expressing bFGF under doxycycline control", *Experimental Neurology,* 247 (2013).

[9] Y. Liang, P. Walczak, J.W.M. Bulte, "The survival of engrafted neural stem cells within hyaluronic acid hydrogels", *Biomaterials,* 34 (2013).

[10] B. Wahlberg *et al.*, "*Ex vivo* biomechanical characterization of syringe-needle ejections for intracerebral cell delivery", *Scientific Reports,* 8 (2018).

[11] A.S. Lee *et al.*, "Prolonged survival of transplanted stem cells after ischaemic injury *via* the slow release of pro-survival peptides from a collagen matrix", *Nature Biomedical Engineering,* 2 (2018).

[12] J. Tchou *et al.*, "Safety and Efficacy of Intratumoral Injections of Chimeric Antigen Receptor (CAR) T Cells in Metastatic Breast Cancer", *Cancer Immunology Research,* 5 (2017).

[13] D.E. Discher, D.J. Mooney, P.W. Zandstra, "Growth Factors, Matrices, and Forces Combine and Control Stem Cells", *Science,* 324 (2009).

[14] L.M. Marquardt *et al.*, "Designer, injectable gels to prevent transplanted Schwann cell loss during spinal cord injury therapy", *Science Advances,* 6 (2021).

[15] S. Chu, N. Uplekar, S. Liu, R. Ghodssi, "Complementary Capillary System Integrated Microneedles for Autonomously Localized Therapeutics Loading", *Journal of Microelectromechanical Systems,* 29 (2020).

[16] S. Liu *et al.*, "Biomimetic Barbed Microneedles for Highly Robust Tissue Anchoring", *IEEE 33rd International Conference on Micro ElectroMechanical Systems (MEMS),* (2020), pp. 885-888.

[17] R. Acevedo *et al.*, "3D Nanoprinted External Microfluidic Structures *Via Ex Situ* Direct Laser Writing", *IEEE 34th International Conference on Micro ElectroMechanical Systems (MEMS)*, (2021), pp. 10–13.

[18] Z. Wen, R. Acevedo, K. Rand-Yain, R.D. Sochol, "3D Nanoprinted Microinjection Needles *Via Ex Situ* Direct Laser Writing", The 25th International Conference on Miniaturized Systems for Chemistry and Life Sciences (MicroTAS), (2021).

CONTACT

*S.Sarker, tel: +1-301-405-6928; ssarker1@umd.edu